Supporting Information

Oliva et al. 10.1073/pnas.1121546109

SI Materials and Methods

Cloning, Protein Expression, and Purification. Phage TubZ was initially cloned into plasmid pDNR-CMV (Clontech) and then subcloned into the NdeI and BamHI sites of a modified pET28 vector that included an N-terminal His tag, followed by a 3C protease site for purification purposes. PCR mutagenesis using this vector as a template generated mutants TubZ-T100A and TubZ-E200A. Genes *cst190* and *cst188* (*tubR* and *tubY*, respectively) were purchased from Genscript USA, Inc. Their sequences were optimized for *E. co*li expression, and both were cloned into NdeI and BamHI sites of vector pET29. PCR mutagenesis using pET29-*cst188* as a template generated TubY truncated proteins $TubY_{226}$ and $TubY_{137}$.

All these proteins were expressed in *E. coli* C41 cells, which were induced at $OD_{600} = 0.6$ by the addition of 1 mM isopropyl-β-D-thiogalactopyranoside. Cells were pelleted, and suspended in 50 mM Tris·HCl and 150 mM NaCl (pH 8.0); 10 μg/mL DNase and 1 mg/mL lysozyme were then added, and cells were opened by sonication. Cell debris was pelleted by centrifugation at 100,000 × *g* for 1 h.

TubZ, TubZ-T100A, and TubZ-E200A were purified by affinity chromatography using HiTrap Chelating columns (GE Healthcare). The His tag was removed (leaving 2 extra N-terminal residues, His-Pro) by incubation with 2 μg/mL N-terminal GST-tagged 3C-protease for 4 h at room temperature in 50 mM Tris·HCl, 150 mM NaCl, 1 mM EDTA, and 1 mM DTT (pH 7.5), and proteins were further purified in a GSTrap FF column (GE Healthcare). TubR was purified by precipitation between 50% and 80% ammonium sulphate saturation, followed by cation exchange chromatography in a HiTrap SP FF column (GE Healthcare) in 50 mM Hepes·KOH, 50 mM KCl, and 1 mM DTT (pH 7.0), in which the protein eluted at 450 mM KCl. $TubY_{226}$ and $TubY_{137}$ were purified by precipitation between 30% and 50% ammonium sulphate saturation, followed by anion exchange chromatography in a HitrapQ HP column (GE Healthcare) using 50 mM Hepes·KOH, 1 mM EDTA, and 1 mM DTT (pH 7.5), where these proteins eluted at 350 mM and 150 mM KCl, respectively. All purifications were followed by size exclusion chromatography in a 1.6-cm × 60-cm Superdex 75 (GE Healthcare) column with 20 mM Tris·HCl, 150 mM KCl, 1 mM EDTA, and 1 mM DTT (pH 7.5). The proteins were then concentrated and stored at −80 °C. Protein concentrations were determined spectrophotometrically, after subtracting any contribution of bound nucleotide, using the extinction coefficients calculated from their sequence (1). Protein integrity was confirmed by mass spectrometry, and protein folding was confirmed by means of CD (Figs. S2*A* and S6*B*).

Crystallization and Structure Determination. TubZ-T100A crystals were grown in 0.1 M Bis-Tris (pH 5.5), 0.1 M ammonium acetate, and 17% PEG 10,000 (Hampton Screen Index) at 22 °C using the sitting-drop, vapor-diffusion technique. Crystals were cryoprotected with 30% 2-methyl-2,4, pentanediol before being mounted in a loop and frozen in liquid nitrogen. An initial dataset was collected at beamline PROXIMA1 (SOLEIL). These data were integrated and reduced using XDS (2) and SCALA (3, 4). The initial coordinates were determined by molecular replacement using the coordinates of *B. subtilis* FtsZ [Protein Data Bank (PDB) ID code 2VAM] in BALBES (5) that correctly placed the N-terminal domain. The C-terminal domain was built using previous coordinates in Auto-Rickshaw (6). Several cycles of refinement using PHENIX (4) and iterative model building with COOT (7) were carried out. High-resolution X-ray diffraction data were collected at beamline ID14he4 European Synchrotron Radiation Facility (ESRF). Data were integrated and reduced as above and used with the previous model in PHASER (8) for the correct localization of the molecule in the asymmetrical unit. The resulting model was refined using simulated annealing in PHENIX (4), which was also used for water picking. The final model was validated using MolProbity (9). Figures were generated using Pymol (Schrödinger).

AUC. Sedimentation velocity and equilibrium experiments were performed at 20 °C (TubR and TubY) or 30 °C (TubZ) in a Beckman Optima XLI analytical ultracentrifuge with absorption and interference optics, using an An50/Ti rotor with 12-mm double-sector centerpieces. All experiments were done in PKE buffer [50 mM piperazine-1,4-bis-2-ethanesulfonic acid (PIPES)·KOH, 100 mM potassium acetate, 1 mM EDTA (pH 6.5)], but experiments with $TubY_{226}$ were also carried in 20 mM Tris·HCl, 150 mM KCl, 1 mM EDTA, and 1 mM DTT (pH 7.5). Velocity experiments were carried out at 38,000 (TubZ), 48,000 (TubR), and 45,000 rpm ($TubY_{226}$ and $TubY_{137}$). TubZ (loading concentrations of 7–50 μM) was also equilibrated in buffer containing 50 μM GDP, 50 μM GTP, or 6 mM magnesium acetate. TubR, $TubY_{226}$, and $TubY_{137}$ were analyzed in a wide range of concentrations (10–100 μM), and *tubS* (0.77 μM) was titrated with TubR (0.5–15 μM). Sedimentation coefficient distribution, c(s), was calculated with SEDFIT 12.1b (10).

Equilibrium experiments were conducted at 20 °C. The samples were centrifuged until reaching equilibrium at speeds of 10,000, 12,000, and 15,000 rpm (TubZ); 22,000 and 26,000 rpm (TubR); 9,000, 10,000, and 12,000 rpm (TubR + *tubS*); 6,000, 8,000, and 18,000 rpm ($TubY_{226}$); and 16,000 and 20,000 rpm ($TubY_{137}$). Data were analyzed using Heteroanalysis 1.1.44 software (11). Binding of TubR to 0.77 μM of S1-114 (*tubS*) was measured from the increment over the buoyant molecular weight of the DNA at increasing protein concentrations (the protein contributes comparatively little to the global absorbance at 260 nm). The average buoyant molecular weight values were measured from the radial concentration gradient, $M_b = d(\ln c)/dr^2 = M(1 - v\rho)\omega^2/2RT$ (where M is the monomer molar mass, v is the partial specific volume, ρ is the solvent density, ω is the angular rotor speed, R is the molar gas constant, and T is the temperature).

TubZ Assembly. TubZ polymerization was monitored by light scattering or sedimentation assays. Light scattering assays were performed at 30 °C as described previously (1). Briefly, aliquots of 5–10 μM TubZ in PKE or PNE [50 mM PIPES·NaOH, 100 mM sodium acetate, 1 mM EDTA, and 1 mM EGTA (pH 6.5)] assembly buffers were placed into a Fluoromax-4 spectrofluorometer cuvette thermostated at 30 °C, and the polymerization was typically started by adding 6 mM magnesium acetate or calcium acetate and 1 mM GTP (or 0.1 mM GMPCPP or 0.1 mM GTP-γ-S). Then, light scattering at 90° was measured using both excitation and emission wavelengths at 350 nm to follow assembly. For sedimentation experiments, samples were prepared in a Thermostat plus (Eppendorf) at 30 °C. TubZ was equilibrated with assembly buffer. Adding magnesium or calcium and nucleotide triphosphate as above started polymerization. After incubation time (which varies according to scattering lag phases), samples were centrifuged at 60,000 rpm for 30 min in a Beckman TLA 100 rotor to pellet TubZ polymers. The su-

pernatants were carefully withdrawn, and the pellets were resuspended in the same volume of buffer. Subsequently, SDS/PAGE gels were run to analyze the amount of protein polymerized (in the pellets) or unassembled (in supernatant), or, alternatively, protein concentrations were measured with the Bio-Rad protein assay kit in multiwell plates using spectrophotometrically calibrated TubZ standards and a Varioskan 377 plate reader at 595 nm.

GTPase and Polymer-Bound Nucleotide Assays. GTP, dilithium salt, and GDP, sodium salt, were from Sigma. GMPCPP, Guanosine-5′-[(alpha,beta)-methyleno] Diphosphate (GMPCP), and GTP-γ-S were from Jena Bioscience. GTP and GMPCPP hydrolysis was monitored by the release of the inorganic phosphate with the malachite green assay (12), whereas GTP-γ-S hydrolysis, as well as the nucleotide bound to the protein polymers, were analyzed by HPLC (1).

EM. TubZ filaments were visualized by negative-stain EM. About 20 μL of sample was applied onto formvar-coated copper grids, incubated for 1 min, and then stained with 2% uranyl acetate. Images were taken at several magnifications using a JEOL 1200EX-II microscope operated at 100 kV and equipped with a Gatan CCD camera.

EMSAs. Before the labeling reaction, PCR products were cleaned using the GeneJET PCR purification kit (Fermentas) and oligonucleotides (Sigma) annealed in 10 mM Tris·HCl, 50 mM NaCl, and 1 mM EDTA (pH 8.0). DNA was labeled at 5′ with [γ^{32}P]-ATP (Hartmann Analytic) by 10 units of T4-polynucleotide kinase (Fermentas) in 1× exchanging reaction buffer (incubated for 30 min at 37 °C). The reaction was stopped by adding 25 mM EDTA, and the enzyme was inactivated by incubation at 75 °C for 10 min. Unbound labeled nucleotides were removed by filtration through Sephadex G50 minicolumns (GE Healthcare). For the binding reaction, variable amounts of protein were diluted in binding buffer [20 mM Tris·HCl, 50 mM KCl, 1 mM EDTA, 5 mM Mg_2Cl, and 5% (vol/vol) glycerol (pH 8.0)] containing 0.2 mg/mL BSA and 50 μg/mL poly deoxyinosinic-deoxycitidilic acid sodium salt (dI-dC). The mixture was preincubated for 30 min at 4 °C; 750 pM radiolabeled DNA was then added, and the mixture was incubated at 25 °C for 20 min, loaded into 6% polyacrylamide gels, and run in 0.5× TBE (45 mM Tris·borate and 1 mM EDTA). Dried gels were exposed overnight to X-ray film at −20 °C and scanned.

CD. Spectra were acquired at 25 °C with a Jasco 810 spectropolarimeter using a 1-mm cell in a thermostated cell holder. Four scans of each sample or buffer (1-nm bandwidth and measurement interval, 20-nm·min^{-1} scan speed, and 4-s time constant) were averaged. CD data (millidegrees) were reduced to mean residue ellipticity values (degrees cm^2·dmol^{-1}) with Jasco J800 software and plotted.

Phylogenetic Analysis. Sequences were collected by means of a BLAST search on the UniProt database using the TubZ/RepX homologs from the c-st phage as the query and the pBtoxis/pOX1 plasmids and E-values of 1.0E-15 as the threshold, typically before archeabacterial homologs appear in the hit list. *Pseudomonas* phage sequences were found by text search, followed by manual analysis, and added to the dataset. We included only nonredundant sequences from different species and homologs from only one species per archeabacterial taxonomic class. Sequences were aligned using MUSCLE (13), and the optimal phylogenetic tree was constructed by the neighbor-joining method (14) utilizing the MEGA 5.0 program (15). The percentage of replicate trees resulting from 1,000 replicates by means of the bootstrap test is displayed at each branch in Fig. 5*B*. The evolutionary distances, in residue substitution per site, were calculated by the Poisson correction method (16) for positions with at least 50% site coverage. Other tree-inferring methods and parameters rendered comparable results.

1. Oliva MA, et al. (2003) Assembly of archaeal cell division protein FtsZ and a GTPase-inactive mutant into double-stranded filaments. *J Biol Chem* 278:33562–33570.
2. Kabsch W (2010) XDS. *Acta Crystallogr D Biol Crystallogr* 66:125–132.
3. Collaborative Computational Project, Number 4(1994) The CCP4 suite: Programs for protein crystallography. *Acta Crystallogr D Biol Crystallogr* 50:760–763.
4. Adams PD, et al. (2010) PHENIX: A comprehensive Python-based system for macromolecular structure solution. *Acta Crystallogr D Biol Crystallogr* 66:213–221.
5. Long F, Vagin AA, Young P, Murshudov GN (2008) BALBES: A molecular-replacement pipeline. *Acta Crystallogr D Biol Crystallogr* 64:125–132.
6. Panjikar S, Parthasarathy V, Lamzin VS, Weiss MS, Tucker PA (2005) Auto-rickshaw: An automated crystal structure determination platform as an efficient tool for the validation of an X-ray diffraction experiment. *Acta Crystallogr D Biol Crystallogr* 61: 449–457.
7. Emsley P, Lohkamp B, Scott WG, Cowtan K (2010) Features and development of Coot. *Acta Crystallogr D Biol Crystallogr* 66:486–501.
8. McCoy AJ, et al. (2007) Phaser crystallographic software. *J Appl Cryst* 40:658–674.
9. Chen VB, et al. (2010) MolProbity: All-atom structure validation for macromolecular crystallography. *Acta Crystallogr D Biol Crystallogr* 66:12–21.
10. Schuck P, Perugini MA, Gonzales NR, Howlett GJ, Schubert D (2002) Size-distribution analysis of proteins by analytical ultracentrifugation: Strategies and application to model systems. *Biophys J* 82:1096–1111.
11. Cole JL (2004) Analysis of heterogeneous interactions. *Methods Enzymol* 384:212–232.
12. Kodama T, Fukui K, Kometani K (1986) The initial phosphate burst in ATP hydrolysis by myosin and subfragment-1 as studied by a modified malachite green method for determination of inorganic phosphate. *J Biochem* 99:1465–1472.
13. Edgar RC (2004) MUSCLE: Multiple sequence alignment with high accuracy and high throughput. *Nucleic Acids Res* 32:1792–1797.
14. Saitou N, Nei M (1987) The neighbor-joining method: A new method for reconstructing phylogenetic trees. *Mol Biol Evol* 4:406–425.
15. Kumar S, Tamura K, Jakobsen IB, Nei M (2001) MEGA2: Molecular evolutionary genetics analysis software. *Bioinformatics* 17:1244–1245.
16. Zuckerkandl E, Pauling L (1965) Molecules as documents of evolutionary history. *J Theor Biol* 8:357–366.

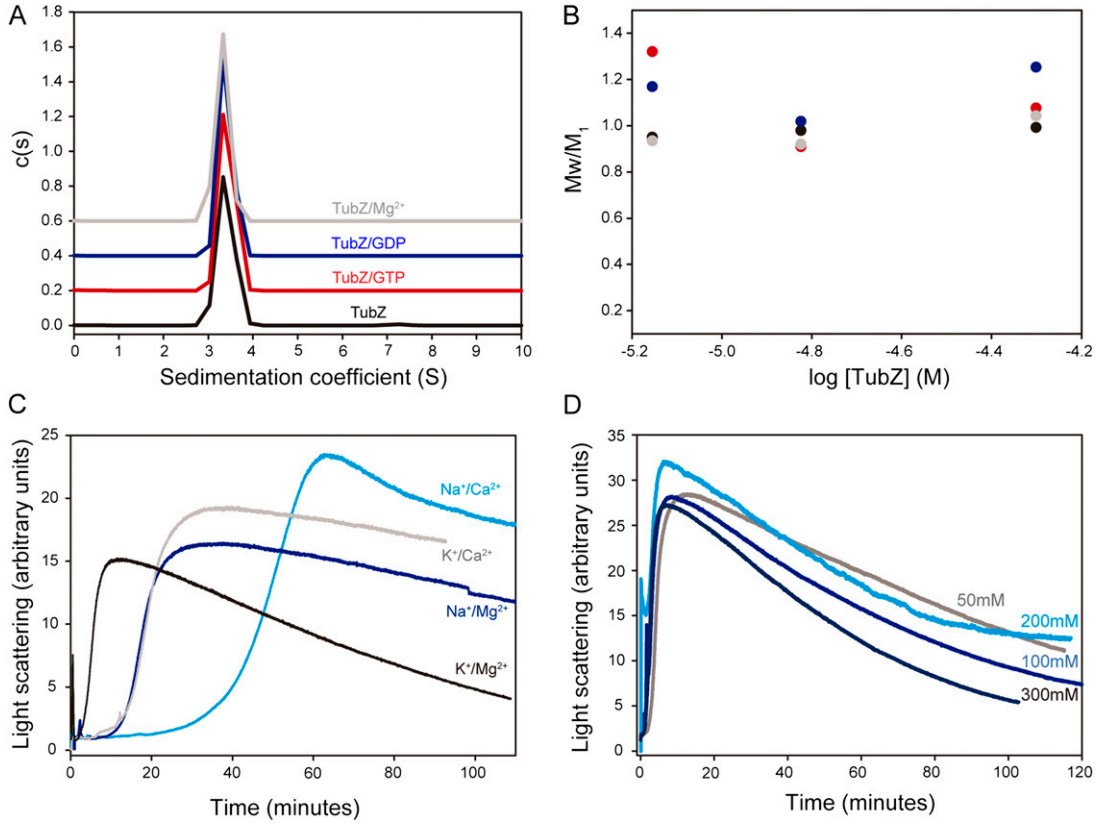

Fig. S1. TubZ characterization. AUC sedimentation velocity (*A*) and equilibrium (*B*) experiments of 15 μM TubZ alone or with nucleotide (50 μM) or magnesium (6 mM). (*C*) TubZ WT assembly monitored by 90° light scattering in PKE (K^+) and PNE [50 mM PIPES NaOH, 100 mM sodium acetate, 1 mM EDTA, 1 mM EGTA (pH 6.5)] (Na^+) with Mg^{2+} or Ca^{2+} as indicated. (*D*) TubZ WT assembly monitored by 90° light scattering in PKE with 50 mM (gray), 100 mM (dark blue), 200 mM (light blue), and 300 mM (black) potassium acetate.

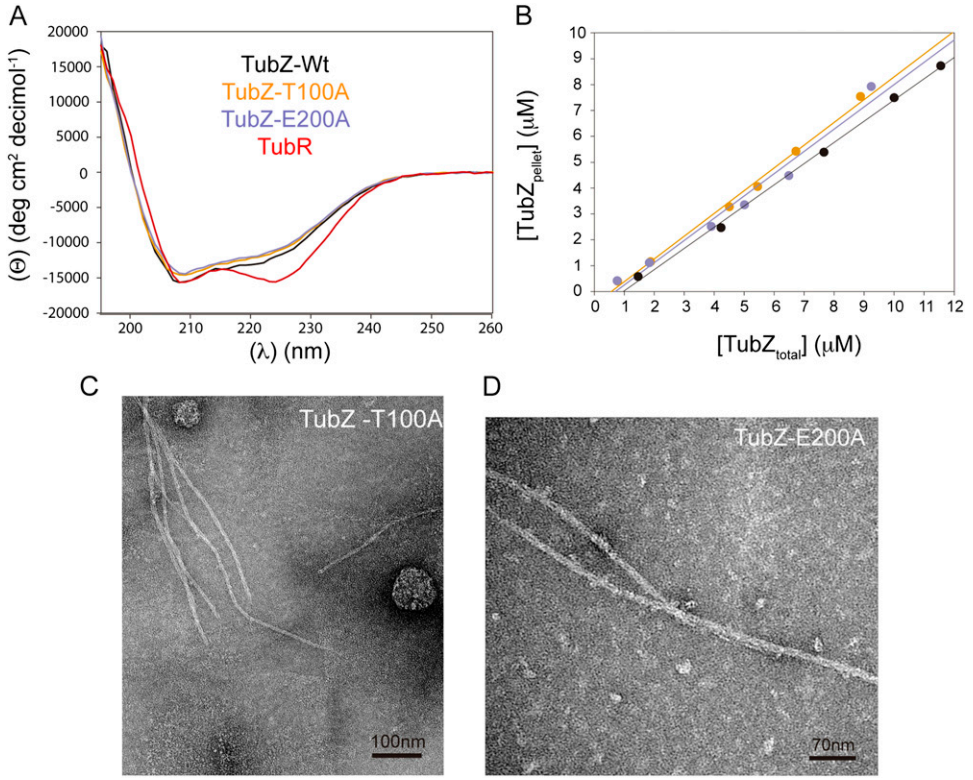

Fig. S2. Characterization of TubZ mutants T100A and E200A and TubR folding. (*A*) Far-UV CD spectra of TubZ WT (black), TubZ-T100A (orange), TubZ-E200A (blue), and TubR (red) at 25 °C show that all these are α/β-proteins that remain folded after purification. (*B*) TubZ WT (black), TubZ-T100A (orange), and TubZ-E200A (blue) critical concentration determination by sedimentation assays. (*C*) Electron micrograph of 10 μM TubZ-T100A assembled in PKE buffer with 1 mM GTP and 6 mM Mg^{2+}. (*D*) Same as in *C* but with TubZ-E200A.

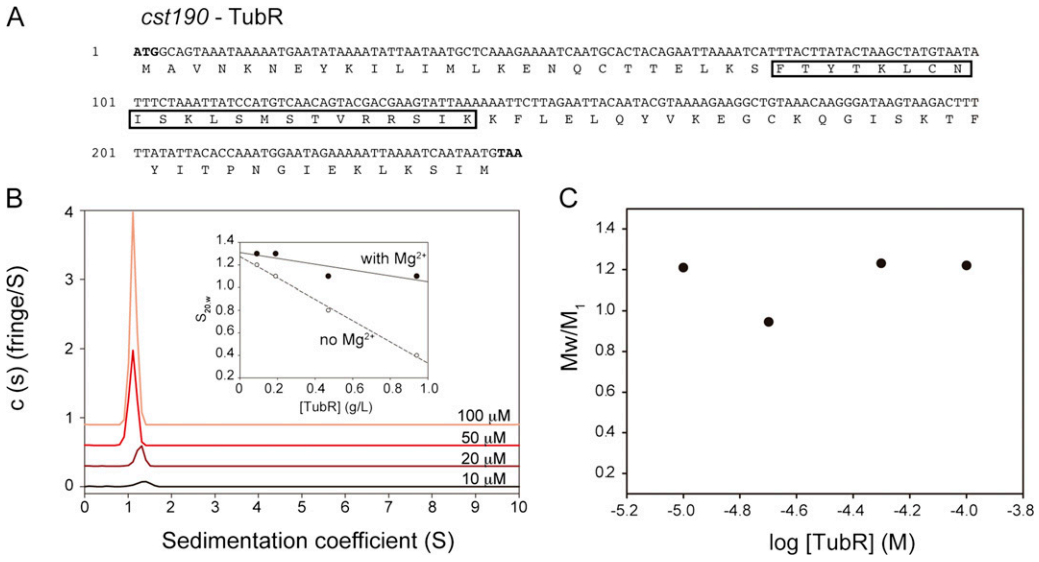

Fig. S3. TubR characterization. (*A*) DNA and translated protein sequence of TubR where the HTH motif is highlighted in a black box. AUC velocity (*B*) and equilibrium (*C*) experiments of TubR in a range of concentrations that show the protein is a monomer. (*B*, *Inset*) $s_{20,w}$ vs. protein concentration for $s^0_{20,w}$ determination.

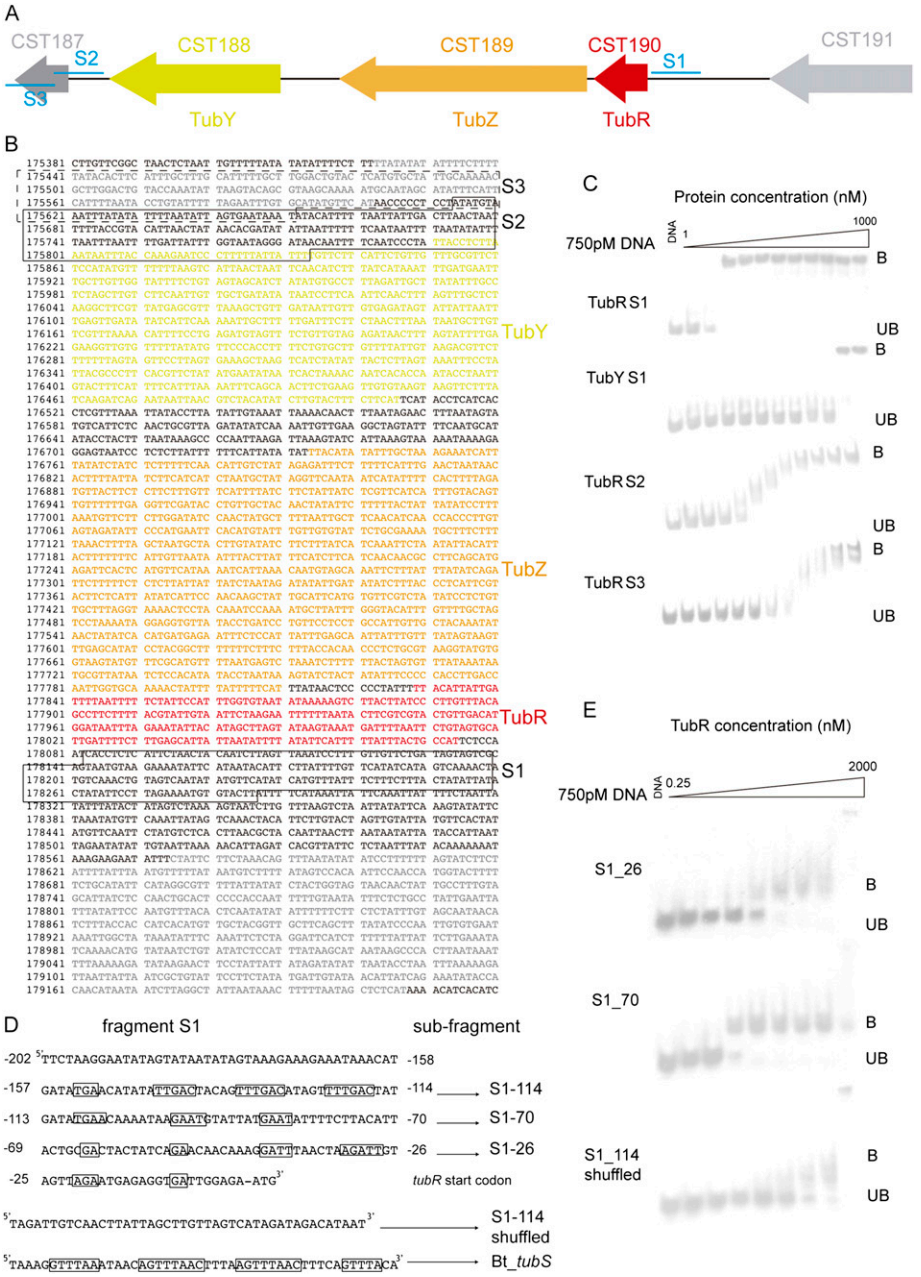

Fig. S4. Localization of the centromere-like sequence *tubS*. (*A*) Schematic representation of the c-st phage gene cluster, including the ORFs CST188 (*tubY*, yellow), CST189 (*tubZ*, orange), and CST190 (*tubR*, red). Highlighted in blue is the localization of the fragments used during the search for the centromere-like sequence *tubS*. (*B*) Phage c-st genomic sequence of the putative partition system cluster localized between 175,791 bp and 178,291 bp, including genes encoding for TubY (yellow), TubZ (orange), and TubR (red), and the centromere-like sequence at fragment S1. Highlighted in boxes are the sequences of the fragments (S1, S2, and S3) used during *tubS* localization. (*C*) EMSA assays using γ-^{32}P–labeled 200-bp fragments S1, S2, and S3 show the DNA shift (B, bound; UB, unbound) attributable to binding of TubR or TubY. (*D*) Sequence (5′—3′) of the 44-bp subfragments within fragment S1 used during *tubS* localization, shuffled subfragment S1-114, and the described centromere-like *tubS* sequence from *B. thuringiensis*. Fully conserved nucleotides shared between adjacent iterons in subfragments S1-26, S1-70, and S1-114 are boxed. We chose this fragment size because there is a clear minimal biletter "AG" motif with a regular periodicity of 11 bp that spans over the first 200 bp upstream of *tubR*. Fourfold repetitions of degenerated sequences of similar length were also reported for other centromere-like regions (1). (*E*) EMSA assays using γ-^{32}P–labeled subfragments S1-26, S1-70, and S1-114 shuffled, which were used as controls to show that binding is highly sequence-specific.

1. Tang M, Bideshi DK, Park HW, Federici BA (2007) Iteron-binding ORF157 and FtsZ-like ORF156 proteins encoded by pBtoxis play a role in its replication in Bacillus thuringiensis subsp. israelensis. *J Bacteriol* 189:8053–8058.

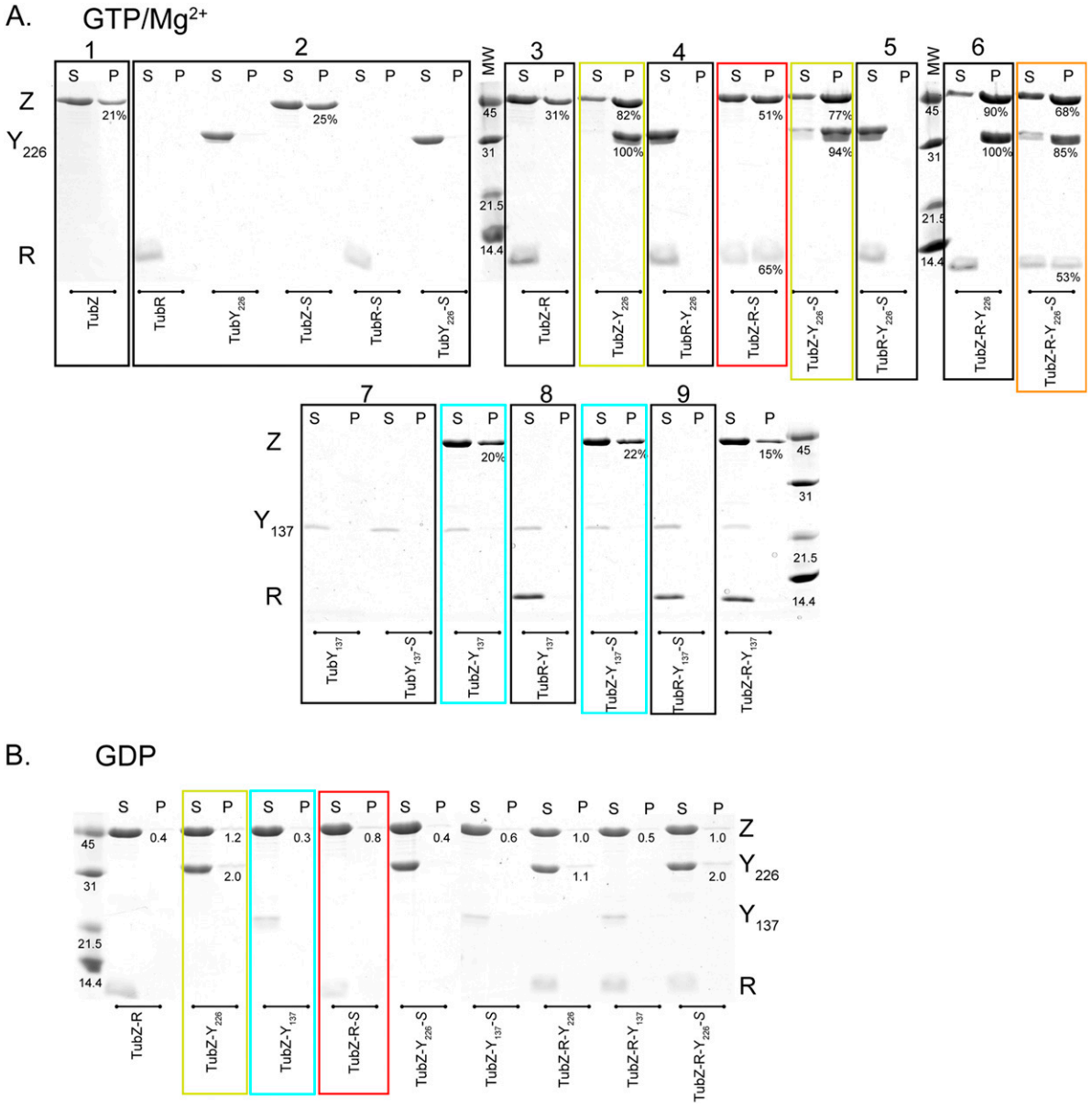

Fig. S5. Cosedimentation experiments. S (supernatant) and P (pellet) fractions were run in the lanes indicated. (*A*) Sedimentation experiments in PKE buffer with 1 mM GTP and 6 mM magnesium acetate at 30 °C of TubZ (10 μM), TubR (20 μM), $TubY_{226}$ (10 μM) or $TubY_{137}$ (10 μM) in the absence and presence of *tubS* (5 μM S1-114). Mixtures were prepared and incubated for at least 10 min before centrifugation at 60,000 rpm in a Beckman TLA-100 rotor for 30 min. Here, we show that (*i*) under TubZ filament assembly conditions (box 1), TubR, $TubY_{137}$, and $TubY_{226}$ did not sediment alone or in the presence of DNA (boxes 2 and 7); (*ii*) TubR binds to TubZ filaments only in the presence of DNA (red box), because there is no cosedimentation when *tubS* is absent (boxes 3 and 6); (*iii*) TubY binds to TubZ filaments through the coiled-coil, because $TubY_{137}$ does not cosediment (blue boxes) and *tubS* is not necessary for the cosedimentation (yellow boxes); (*iv*) TubR and TubY do not cosediment in the presence or absence of DNA (boxes 4, 5, 8, and 9); and (*v*) the three proteins cosedimented in the presence of DNA (orange box). (*B*) Control sedimentation experiments under the same conditions as in *A* but with GDP and no magnesium, such that TubZ does not assemble into filaments. Here, we show that there is no sedimentation of TubR-*S* (red box), $TubY_{226}$ (yellow box), or $TubY_{137}$ (blue box).

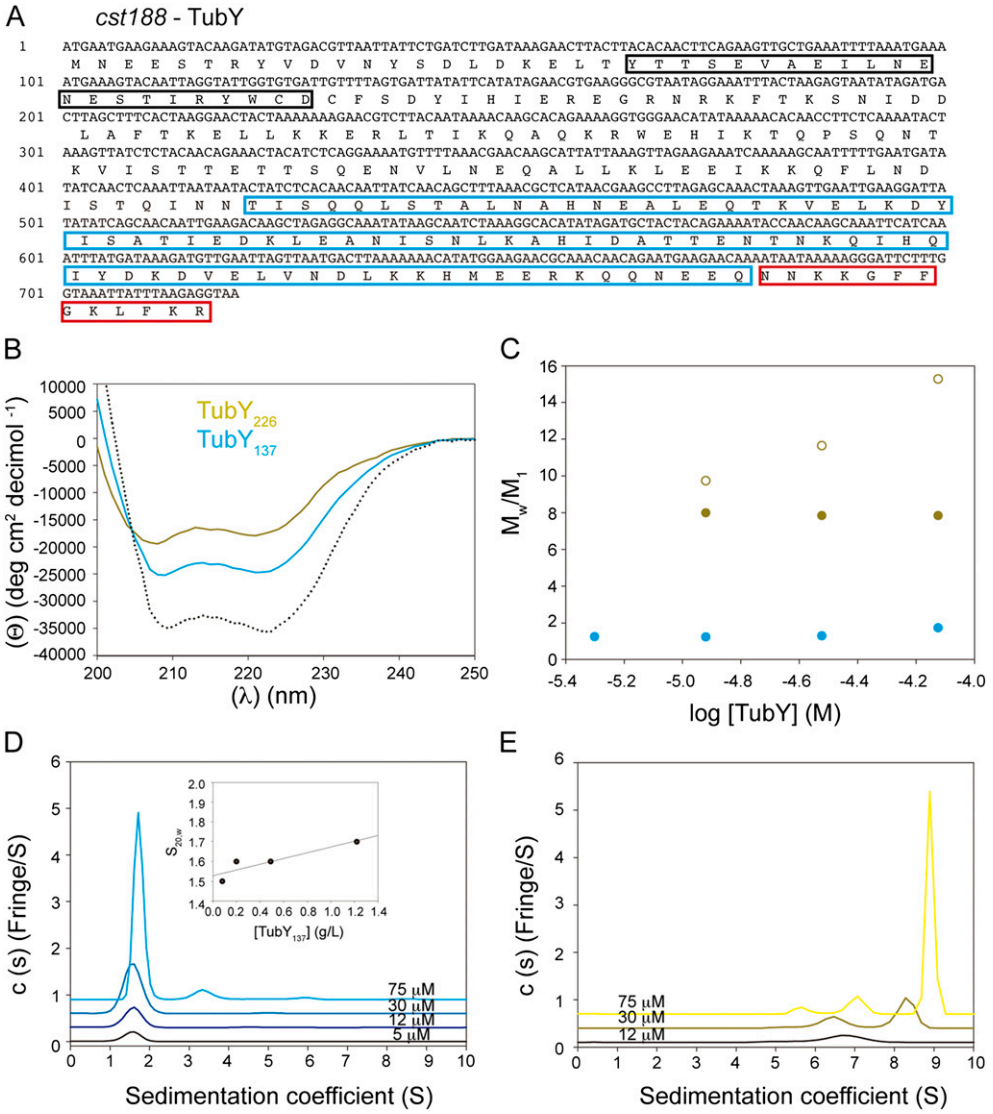

Fig. S6. TubY characterization. (*A*) DNA and translated protein sequence of TubY where the HTH motif is highlighted in a black box, the predicted coiled-coil is highlighted in a blue box, and the C-terminal tail is highlighted in a red box. (*B*) Far-UV CD spectra of $TubY_{137}$ (blue) and $TubY_{226}$ (yellow) at 25 °C show that both proteins are folded after purification. The dotted line is the theoretical spectrum calculated for the $TubY_{138–226}$ segment, obtained by subtracting the molar ellipticity of spectra of $TubY_{137}$ from $TubY_{226}$. The resulting curve represents an ∼100% α-helical spectrum with a deeper minimum at 222 nm, characteristic of coiled-coils (1, 2). (*C*) AUC equilibrium experiments of $TubY_{137}$ (blue) and $TubY_{226}$ (yellow) in a range of concentrations. $TubY_{226}$ experiments were carried out in 20 mM Tris·HCl, 150 mM KCl, 1 mM EDTA, and 1 mM DTT (pH 7.5) buffer (solid circles), where this protein forms well-defined octamers, and in PKE buffer (empty circles), where there are larger oligomers. (*D*) AUC velocity experiments of $TubY_{137}$ in a range of concentrations. (*Inset*) $s_{20,w}$ values vs. protein concentration. (*E*) Sedimentation velocity of $TubY_{226}$ in 20 mM Tris·HCl, 150 mM KCl, 1 mM EDTA, and 1 mM DTT (pH 7.5) buffer.

1. Lau SY, Taneja AK, Hodges RS (1984) Synthesis of a model protein of defined secondary and quaternary structure. Effect of chain length on the stabilization and formation of two-stranded alpha-helical coiled-coils. *J Biol Chem* 259:13253–13261.
2. Zhou NE, Kay CM, Hodges RS (1992) Synthetic model proteins. Positional effects of interchain hydrophobic interactions on stability of two-stranded alpha-helical coiled-coils. *J Biol Chem* 267:2664–2670.

Table S1. Data collection and refinement statistics

Protein	TubZ-T100A
Data collection	
Space group	C2
Cell dimensions	
a, *b*, *c*; Å	104.99, 85.61, 44.94
α, β, γ; °	90.00, 93.87, 90.00
Resolution, Å	44.83–2.30
R_{merge}*	0.055 (0.42)
I/σ(I)*	9.8 (1.9)
Completeness, %*	95.5 (73.4)
Redundancy	7.2 (5.4)
Refinement	
Resolution, Å	2.3
No. reflections	16,842
R_{work}/R_{free} †	0.17/0.22
No. atoms	2,460
Protein	2,395
Water	59
B-factor	
Protein	51.83
Water	45.54
rmsd	
Bond lengths, Å	0.007
Bond angles, °	0.980

*Highest resolution shell is shown in parentheses.
†For determination of Rfree, 5% of reflections were randomly selected before refinement.

Table S2. TubZ filament biochemical properties

	Cc, μM	Assembly lag, min	GTPase, min^{-1}	Polymer GDP, %
K^+/Mg^{2+} (standard, WT)	0.97	2	0.97	96
TubZ-T100A	0.56	10	0.07	79
TubZ-E200A	0.70	40	0.11	16
GMPCPP	0.29	10	0.05	—
GTP-γ-S	0.71	10	0.18	—
Na^+/Mg^{2+}	0.84	10	0.5	98
Na^+/Ca^{2+}	0.94	35	0.02	88
K^+/Ca^{2+}	1	10	0.32	91

Cc, critical concentration.